nature genetics

Supplementary information

https://doi.org/10.1038/s41588-025-02281-4

Natural variation in *SBRR1* shows high potential for sheath blight resistance breeding in rice

In the format provided by the authors and unedited

Table of Contents

Supplementary note 1: Identification of candidate gene *SBRR1* in the linkage disequilibrium block

According to the 5 single nucleotide polymorphisms (SNPs) in the linkage disequilibrium (LD) block, four haplotypes were identified and, based on their phenotypes, the two most significant SNPs were found to have a dominant contribution to resistance (Supplementary Fig. 1a,b; Supplementary Table 1). In this LD block, 24 genes were annotated, in which only *LOC_Os11g10290*, encoding a G-type LecRLK (lectin receptor-like kinase) protein, strongly responded to *R. solani* infection when assessed by reverse transcription-quantitative PCR (RT-qPCR) (Supplementary Fig. 1c,d). This gene was named *ShB Resistance RLK1* (*SBRR1*) hereafter. Interestingly, the two most significant SNPs are located in the promoter and coding regions of *SBRR1*, respectively (Supplementary Fig. 1a).

Supplementary note 2: *SBRR1* positively regulates ShB resistance

To validate the involvement of *SBRR1* in rice ShB resistance, we identified a T-DNA insertion mutant with the *SBRR1* gene disrupted in the background of *japonica* variety Dongjin (DJ, carrying *SBRR1-S*) and confirmed that the T-DNA insertion at a location 19 bp downstream of the *SBRR1* start codon resulted in the loss of function of *SBRR1* (hereafter named *sbrr1*) (Extended Data Fig. 2a-d). In field inoculation assays, we found that the *sbrr1* mutant was clearly more susceptible to sheath blight (ShB) with disease scores of 7.38 compared with wildtype (WT, 6.09) (Extended Data Fig. 2e). We then knocked out *SBRR1* in the DJ background via CRISPR/Cas9-mediated genome editing and obtained three knockout lines (*sbrr1-ko1/2/3*) carrying different sequence variations (Supplementary Fig. 2). The three knockout lines all displayed higher susceptibility (lesion lengths 23.27~25.59 cm) than WT (18.16 cm) (Fig. 2a; Supplementary Fig. 3). We further transformed DJ with overexpression (OE) construct pUbi:$SBRR1^{DJ}$ (maize *ubiquitin* promoter driving *SBRR1-S* coding region from DJ). The three OE lines all clearly showed much higher *SBRR1* transcript levels than WT with or without *R. solani* inoculation (Supplementary Fig. 2), and displayed significantly shorter lesion lengths (~15cm) than WT (18.3 cm) (Fig. 2b; Supplementary Fig. 3), confirming the importance of *SBRR1* expression level on ShB resistance. We also tested ShB resistance of these transgenic lines in the field and obtained a consistent trend as that in greenhouse (Supplementary Fig. 4a). Notably, no visible changes on major agronomic traits were found in the knockout or OE transgenic lines compared with WT (Supplementary Fig. 4b). These data indicate that *SBRR1* functions as a positive regulator of ShB resistance in rice.

Supplementary note 3: SBRR1 kinase activity is required for its resistance

We conducted a complementation test for *SBRR1* by transforming the *sbrr1* mutant with p*SBRR1*^{DJ}:*SBRR1*^{DJ}. Since *SBRR1* encodes a kinase protein, we also created a kinase dead construct (p*SBRR1*^{DJ}:*SBRR1*^{K553E}) by mutating the conserved lysine (Lys553), located in the ATP binding region of the kinase domain of SBRR1, to glutamate and transformed it into the *sbrr1* mutant. In *in vitro* kinase assay, we found that wild type SBRR1-ICD (ICD, intracellular domain), but not SBRR1-ICD^{K553E}, was autophosphorylated (Fig. 2c), indicating that SBRR1 is an active kinase protein and Lys553 is necessary for its activity. Inoculation assays showed that transgenic lines complemented by wildtype (Com), but not by kinase-dead (KiD), rescued the susceptible phenotype of *sbrr1* mutant, demonstrating that SBRR1 kinase activity is required for its resistance (Fig. 2d; Supplementary Fig. 3).

Supplementary note 4: Differential presence of *SBRR1-R* in *indica* and *japonica* rice varieties

In order to assess the distribution of this elite allele in rice, we analyzed the complete genome information of 85 rice varieties (including 5 wild rice accessions)[1] and identified a SNP (SNP$^{G/A}$) located only 40 bp away from Indel-946 in both wild rice accessions and cultivated rice varieties, in which the SNP^{G} was linked with the functional 256-bp insertion while SNP^{A} was linked with the deletion (Supplementary Fig. 6). To validate their linkage, we further analyzed 430 rice varieties with Illumina sequencing depth over 20x from the 3K rice genome resource[2]. The results showed that, except for 25 varieties with incomplete sequencing coverage in the target region, the remaining 405 varieties all showed that SNP^{G} was completely linked with the functional 256-bp insertion (Supplementary Table 5). Furthermore, we assessed the distribution of SNP$^{G/A}$ in cultivated rice from the 3K rice genomes project and noticed that the distribution of SNP$^{G/A}$ is uneven between *indica* and *japonica* subspecies (Supplementary Table 6; Supplementary Fig. 7a, χ^2 = 1773.7, P < 0.0001). The vast majority of *indica* varieties (1422 out of 1686, 84.34%) possess the *SBRR1-R* allele, whereas most of *japonica* varieties (734 out of 792, 92.68%) contain the *SBRR1-S* allele (Supplementary Fig. 7a). The estimated parameter values of genetic divergence between the two rice subspecies are relatively higher in the *SBRR1* locus than in its flanking genomic regions (Supplementary Fig. 7b), indicating the genetic differentiation of *SBRR1* between *indica* and *japonica* subspecies.

Supplementary note 5: SIP1 interacts with SBRR1 and is required for SBRR1-mediated ShB resistance.

To elucidate the signaling of *SBRR1*-mediated ShB resistance, we performed yeast two-hybrid (Y2H) screens with the SBRR1-ECD (ECD, extracellular domain) and SBRR1-ICD protein as baits separately, and obtained a cDNA of *LOC_Os03g63480* that encodes an ankyrin (ANK)-repeat domain protein. Subsequently, this protein, named SBRR1-interacting protein 1 (SIP1), was verified for interaction with SBRR1-ECD in a Y2H assay and an *in vitro* GST (glutathione S-transferase) pull-down assay (Fig. 6a, b). In order to double check the *in vivo* interaction between SBRR1 and SIP1 in rice, we developed an antibody against SIP1. We conducted a co-immunoprecipitation test using total protein extracted from *SBRR1*-OE1 (SBRR1 tagged with FLAG) plants and clearly observed that SIP1 was co-immunoprecipitated with SBRR1-FLAG from rice total protein (Fig. 6c).

To investigate the function of SIP1 in ShB resistance, we generated three independent *SIP1* knockout (*sip1-ko*, carrying either a single-base insertion or an 8-base deletion) lines via CRISPR/Cas9 technology and three overexpression (*SIP1*-OE1) lines (Supplementary Fig. 10) in DJ background and evaluated their ShB resistance. We found that the *sip1-ko* lines (*sip1-ko-1/2/3*) showed significantly longer ShB lesions (21.02-21.78 cm) than WT (18.11cm), whereas *SIP1*-OE lines (*SIP1*-OE1/2/3) showed significantly shorter lesions (15.69-16.23 cm) (Fig. 6d), indicating that *SIP1*, like *SBRR1*, positively regulates ShB resistance in rice.

To explore the role of *SIP1* in *SBRR1*-mediated resistance signaling, we crossed *sbrr1-ko1* with *SIP1*-OE1 line, *SBRR1*-OE1 with *sip1-ko1* line, and *sbrr1-ko1* with *sip1-ko1* to develop *sbrr1-ko1/sip1-ko1*, *sbrr1-ko1*/*SIP1*-OE1, and *SBRR1*-OE1/*sip1-ko1* homozygous lines (Supplementary Fig. 11). Assessment of ShB resistance showed that *SIP1*-OE plants displayed significantly enhanced resistance compared with WT plants, but were slightly less resistant than *SBRR1*-OE plants (Fig. 6e). Double-knockout *sbrr1-ko1/sip1-ko1* plants and single-knockout *sbrr1-ko1*, *sip1-ko1*, and *sbrr1-ko1/SIP1*-OE1 plants all showed similar ShB susceptible levels, but all were significantly more susceptible than WT, suggesting that the resistance conferred by *SIP1* depends on *SBRR1*. In addition, *SBRR1* overexpression in *sip1-ko1* background (*sip1-ko1/SBRR1*-OE1) restored *sip1-ko1* to a resistance level similar to the WT level, but lower than that of *SBRR1*-OE1, demonstrating that the function of *SBRR1* partially relies on *SIP1* (Fig. 6e). These data demonstrate that SIP1 plays a vital role in SBRR1-mediated ShB resistance.

Supplementary note 6: Additional methods and materials

Plasmid construction and rice transformation

For CRISPR/Cas9 knockout construction, oligonucleotides containing an 18-bp gene-specific sequence of *SBRR1/SIP1/Chit3/Chit4/ bHLH57* (basic helix-loop helix 57) were synthesized and annealed to form the oligo adaptors. The oligo adaptors were firstly cloned into entry vector pOs-sgRNA, then subcloned into Gateway destination vector pOs-Cas9 (ref. 3). To prepare overexpression constructs, the *SBRR1*/*SIP1*/*Chit3/bHLH57* coding regions of DJ were individually inserted into the pCubi1390-3×FLAG vector under control of the maize ubiquitin promoter. For genetic complementation, a 2,954 bp promoter fragment and the 2,463 bp coding region of *SBRR1* from DJ were fused and inserted into the pCAMBIA2300 binary vector to generate the p*SBRR1*^{DJ}:*SBRR1*^{DJ} construct. Similarly, plasmids p*SBRR1*^{DJ}:*SBRR1*^{K553E} and p*SBRR1*^{XWX7}:*SBRR1*^{DJ} (*SBRR1* from DJ driven by the 3,341 bp *SBRR1* promoter from Xiangwanxian 7 (XWX7)) were also constructed. Subsequently, the constructs were introduced into *Agrobacterium tumefaciens EHA105* and used to infect rice calli by *Agrobacterium*-mediated transformation method[4]. All primer sequences used are listed in Supplementary Table 13.

RNA extraction and RT-qPCR

Total RNA was extracted from rice leaf sheaths using the TRIzol reagent (Invitrogen, Carlsbad, CA). First-strand cDNA was reverse-transcribed from 1 μg of purified total RNA following the manufacturer's protocol (PrimeScript™ 1st Strand cDNA Synthesis Kit, TaKaRa). RT-qPCR was performed with gene-specific primers using a SYBR Premix ExTaq Ⅱ kit (Takara) on the CFX96TM Real-Time PCR Detection System (BioRad, Hercules, CA) (Supplementary Table 13). *OsACTIN* was used as the endogenous reference to normalize all RT-qPCR data.

Two-phase Partitioning

Rice tissues were harvested from leaves of 14-day-old *SBRR1*-OE1 and *SBRR1*-OE-1/*sip1-ko1* plants and homogenized with homogenization buffer (25mM Tris [pH7.5], 2mM DTT, 2mM EDTA, 0.5% BSA, 0.25M sucrose, 10% glycerol, 0.1% β-mercaptoethonol and proteinase inhibitor cocktail). The homogenate was centrifuged at 12,000g for 20 min at 4 °C to collect the supernatant. The supernatant was centrifuged at 136,955 g for 90 min at 4 °C to yield microsomal (pellet) and soluble (supernatant) protein fractions. A polyethylene glycol–dextran aqueous two-phase partitioning system was used to separate endomembranes (EMs) and plasma membrane (PM). The microsomal pellets were re-suspended using suspension

medium (250 mM sucrose, 2 mM Tris [pH6.5], 1mM DTT and 0.2% BSA) and subjected to two-phase partitioning. The lower phase (EMs-enriched) and the upper phase (PM-enriched) were partitioned with buffers of lower phase (L, endomembrane fraction) and upper phase (U, PM fraction), respectively. The PM and EM fractions were harvested by centrifugation at 100,620 g for 60 min at 4 °C and re-suspended using suspension medium. Equal amounts of the samples were analyzed by SDS-PAGE and Western blotting. Anti-HSP82 (Beijing Protein Innovation, AbM51099-31-PU; 1:3000 in PBS) and anti-PIP1;1 (Beijing Protein Innovation; AbP80089-A-SE; 1:3000 in PBS) were used as cytoplasmic and PM protein markers, respectively. HRP-conjugated anti-mouse IgG (EASYBIO, BE0102; 1:3000 in PBS) were used as the secondary antibodies.

Supplementary References:

1. Zhang, F. et al. Long-read sequencing of 111 rice genomes reveals significantly larger pan-genomes. *Genome Res.* **32**, 853-863 (2022). https://doi.org:10.1101/gr.276015.121

2. Wang, W. et al. Genomic variation in 3,010 diverse accessions of Asian cultivated rice. *Nature* **557**, 43-49 (2018). https://doi.org: 10.1101/gr.276015.121

3. Miao, J. et al. Targeted mutagenesis in rice using CRISPR-Cas system. *Cell Res.* **23**, 1233-1236 (2013). https://doi.org: 10.1038/cr.2013.123

4. Hiei, Y. Ohta, S. Komari, T. & Kumashiro, T. Efficient transformation of rice (*Oryza sativa* L) mediated by Agrobacterium and sequence analysis of the boundaries of the T-DNA. *Plant J.* **6**, 271-282 (1994). https://doi.org: 10.1046/j.1365-313X.1994.6020271.x

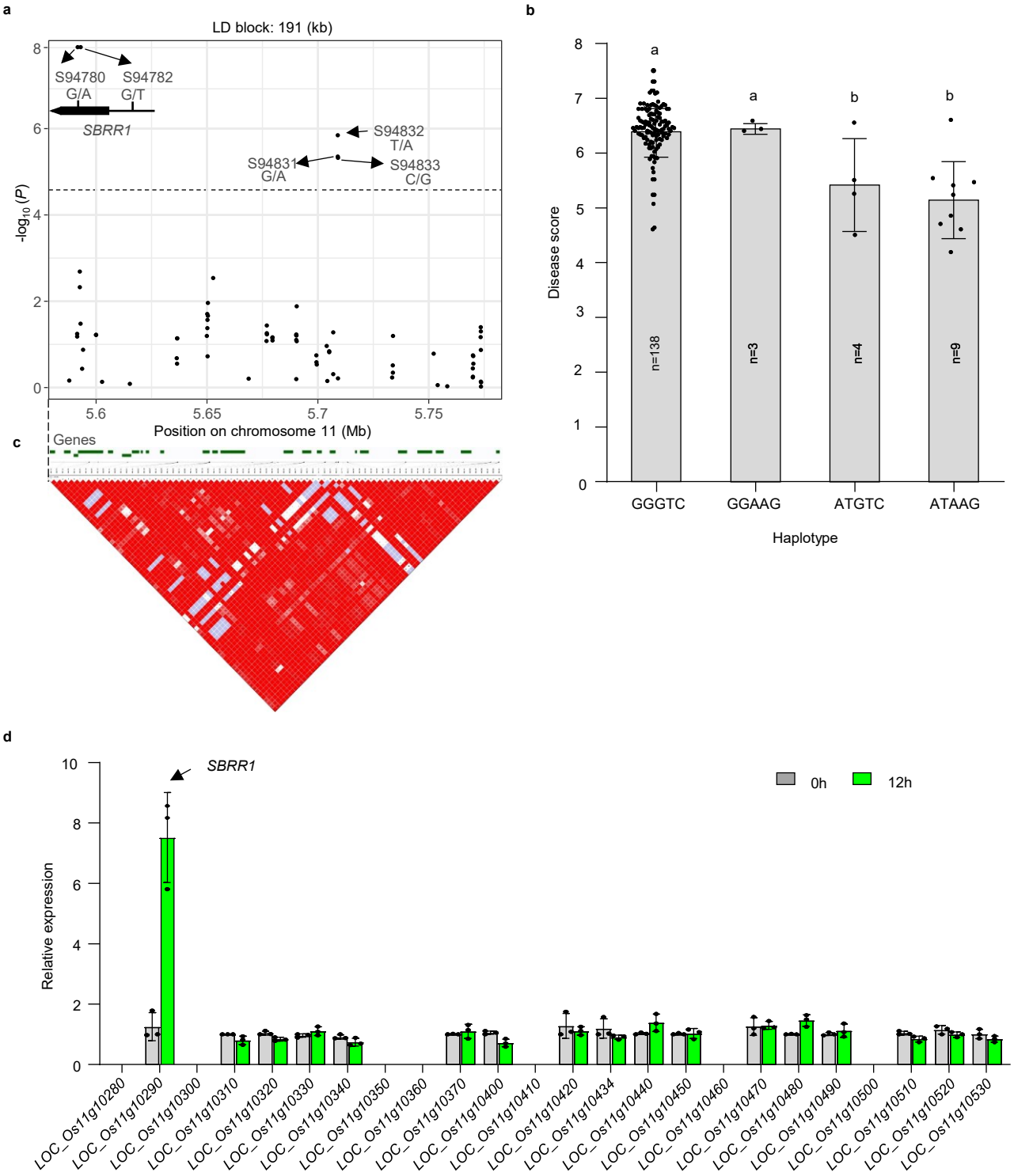

Supplementary Fig. 1. Only *SBRR1* strongly responds to *R. solani* infection in a LD block that includes five significant SNPs. a, Local Manhattan plot for the LD block (191 kb) that includes five significant SNPs (S94780, S94782, S94831, S94832 and S94833). b, Resistance effects of different haplotypes formed by the five significant SNPs. Different lowercase letters indicate significant differences ($P < 0.05$) based on one-way ANOVA with Duncan's multiple range tests. c, LD heatmap and annotated genes in the block. d, Expression levels of the 24 genes in the block in variety XWX 7 in response to *R. solani* infection (n=3). The values in b and d represent mean ± s.d.

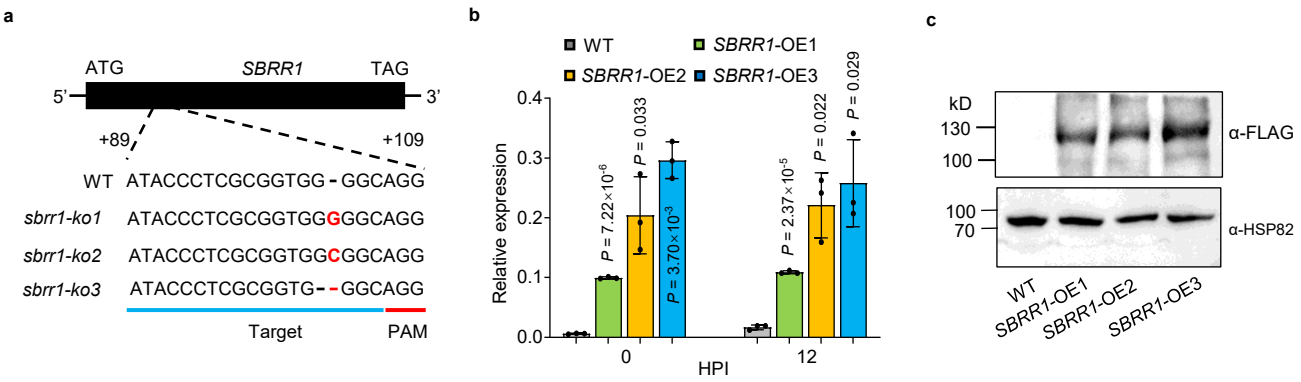

Supplementary Fig. 2. Identification of *SBRR1* knockout lines and overexpression lines. a, Location and sequences of the mutations in *SBRR1* knockout lines (*sbrr1-ko1/2/3*)(a). PAM, protospacer adjacent motif. b, RNA expression levels of *SBRR1* in *SBRR1* overexpression lines (*SBRR1*-OE1/2/3). RNA levels were determined by RT-qPCR. The values represent mean ± s.d (n=3). Statistical significances were determined by a two-sided Student's *t* test. HPI, hours post inoculation. c, Protein levels of SBRR1 in *SBRR1* overexpression lines. HSP82 was used as a loading reference.

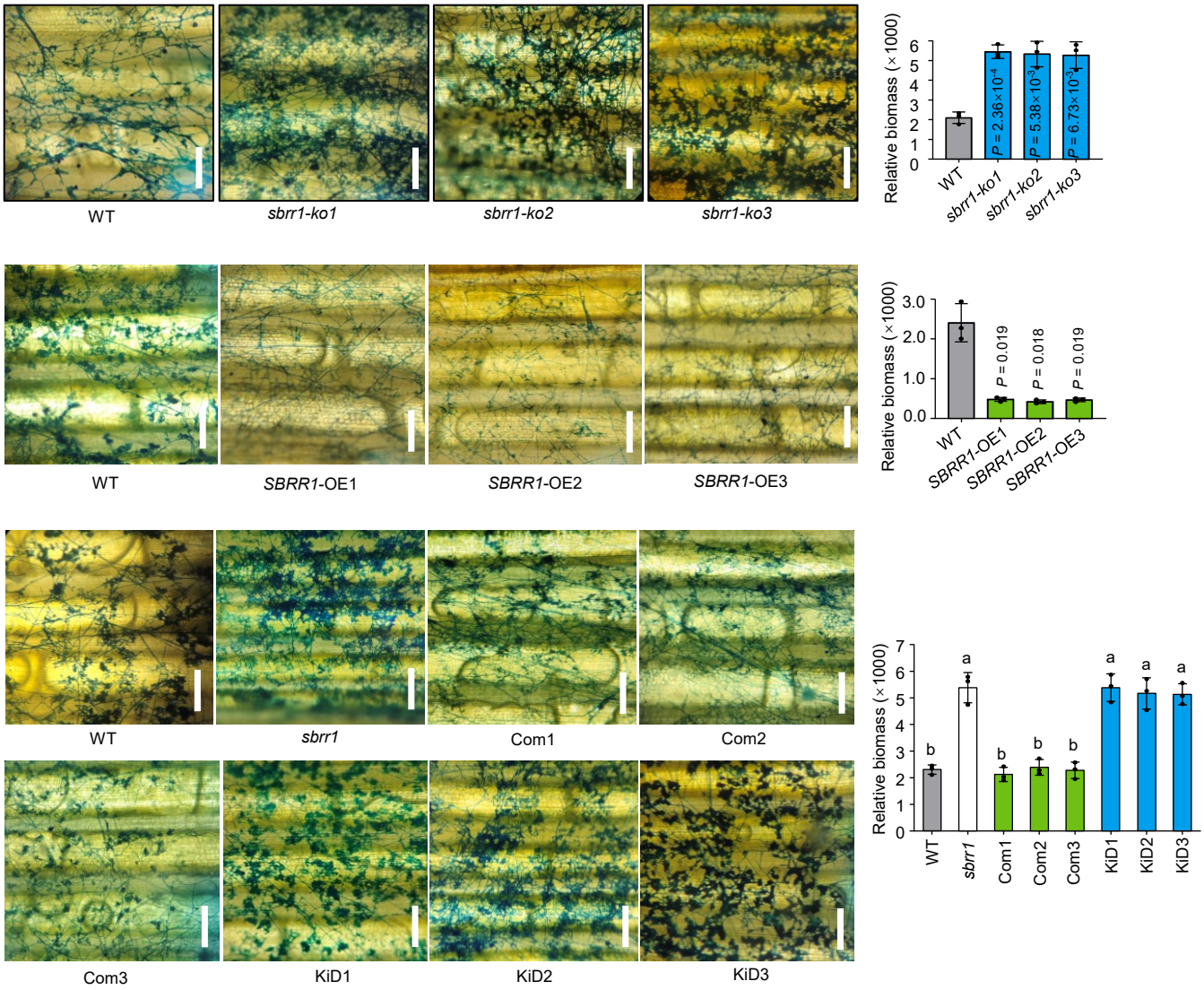

Supplementary Fig. 3. Lactophenol cotton blue staining and relative abundance of *R. solani* biomass in *SBRR1*-related transgenic lines. Lactophenol cotton blue staining shows the hyphae of *R. solani* at the inoculation sites in leaf sheaths. Relative abundance of *R. solani* biomass in the infected leaf sheath was measured by quantitative PCR using specific primers for the 18S rRNA gene of *R. solani*. The *OsActin* gene was used as the reference. The values represent mean ± s.d (n=3). Statistical significances were determined by a two-sided Student's *t* test. Different lowercase letters indicate significant differences ($P < 0.05$) based on one-way ANOVA with Duncan's multiple range tests. Scale bar, 1mm.

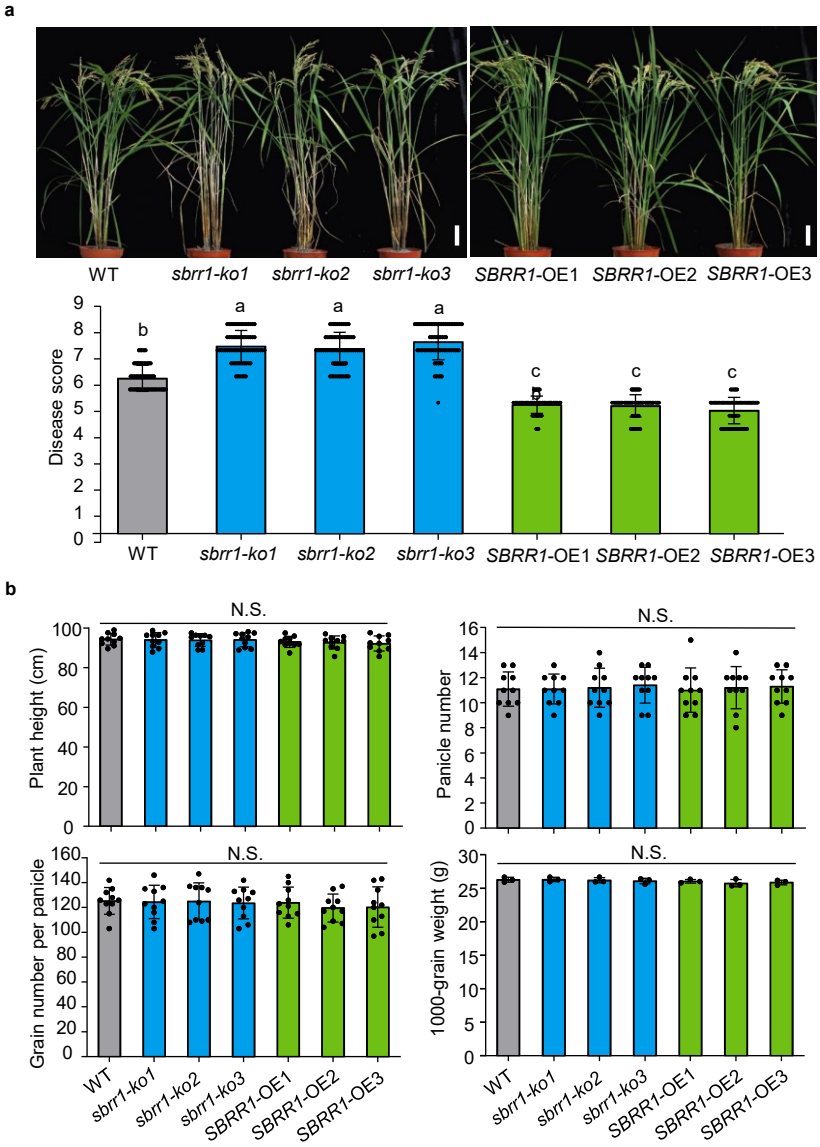

Supplementary Fig. 4. ShB disease scores (a) and main agronomic traits (b) of *SBRR1* knockout (ko) and overexpression (OE) lines in field tests. The values represent mean ± s.d (Disease score, n=72; Plant height, panicle number and grain number per panicle, n=10; 1000-grain weight, n=3). Different lowercase letters in a indicate significant differences ($P < 0.05$) based on one-way ANOVA with Duncan's multiple range tests. N.S. indicates no significant differences. Scale bar, 10 cm.

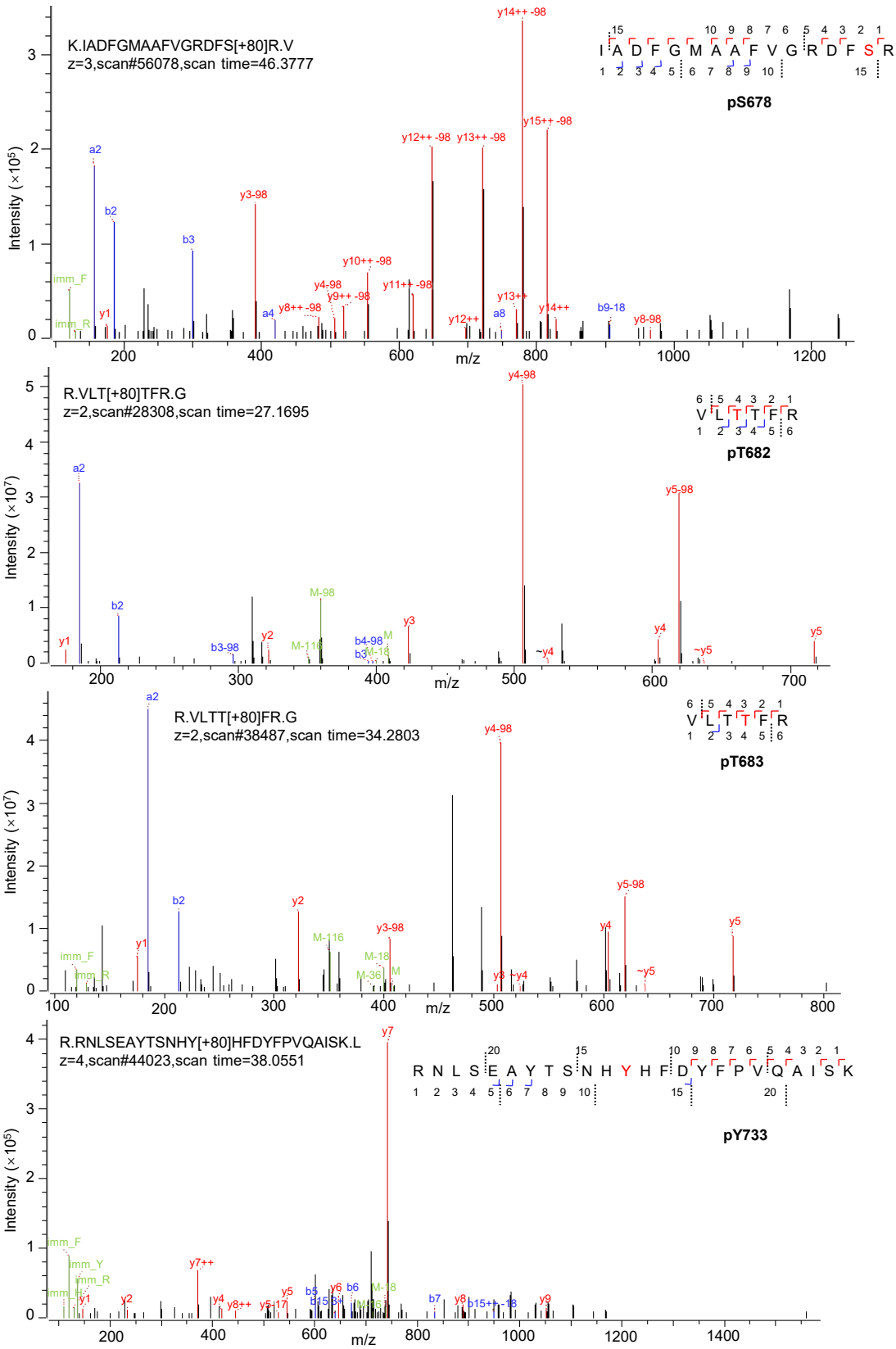

Supplementary Fig. 5. Identification of four phosphorylation sites (S678, T682, T683 and Y733) in SBRR1 protein after *R. solani* attack by quantitative mass spectrometry analysis. The b and y ions are marked in spectra with respective peptide sequence above the spectrum.

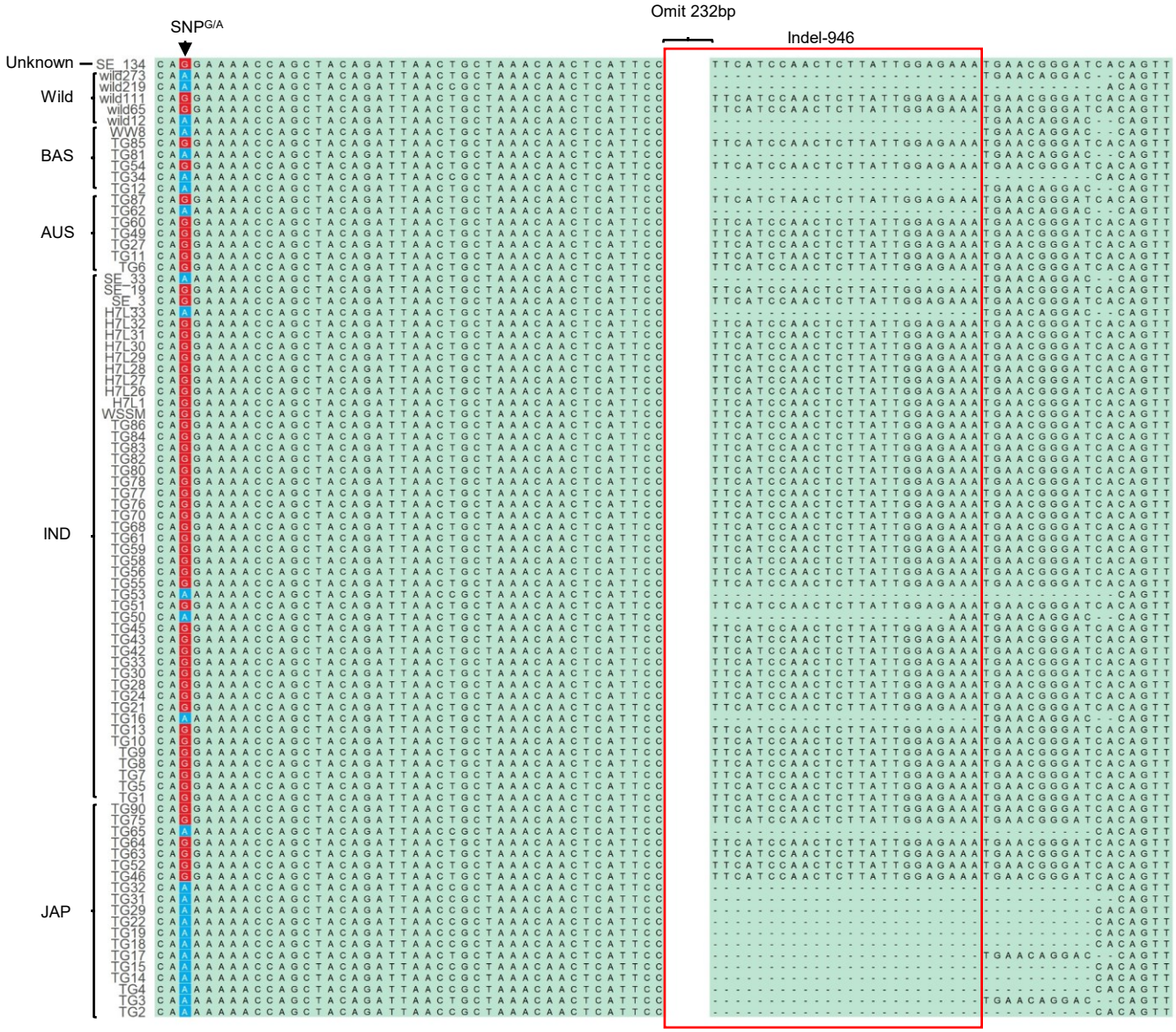

Supplementary Fig. 6. The Indel-946 region in *SBRR1* promoters is completely linked to SNP$^{G/A}$. The red box represents the Indel-946 region and the arrow indicates SNP$^{G/A}$.

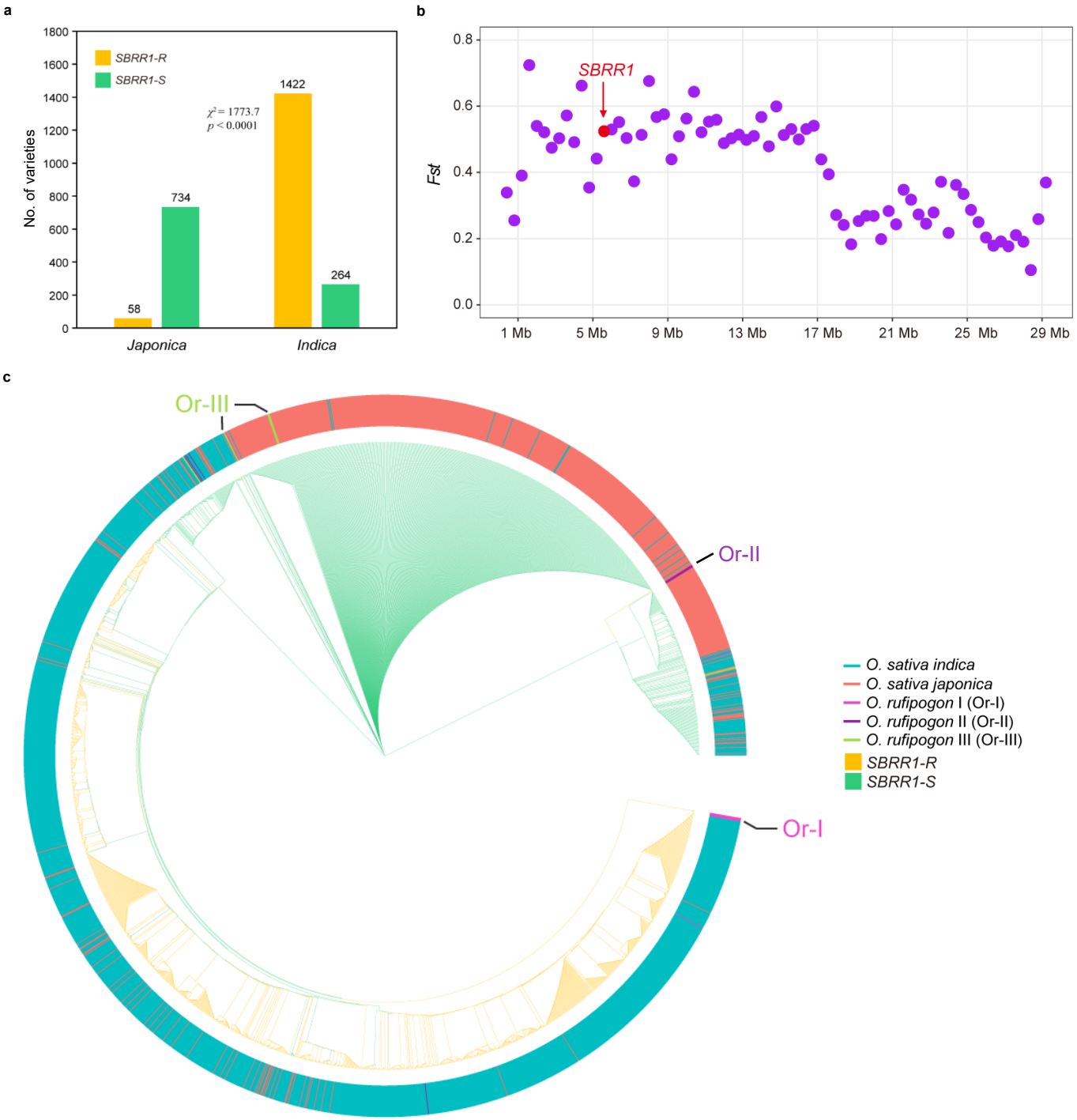

Supplementary Fig. 7. Genetic differences between *SBRR1-R and SBRR1-S* and their phylogenetic relationship in rice. a, The distribution of *SBRR1-R* and *SBRR1-S* alleles is uneven in *japonica* and *indica* varieties. Statistical analysis was performed by the chi-square (χ^2) test. b, Parameter of genetic difference between *indica* and *japonica* for *SBRR1* and its flanking genomic regions. The population-differentiation statistics (F_{ST}) was estimated in each 400-kb window across rice chromosome 11. Red dots indicate the *SBRR1* locus. c, Phylogeny generated from the coding and upstream 1.5-kb sequences of *SBRR1* in both cultivated rice varieties and common wild rice. Outer circle of the tree indicates various rice populations. Inner circle of the tree indicates *SBRR1-R* and *SBRR1-S* alleles. Circle size of the network is proportional to the number of samples for each haplotype.

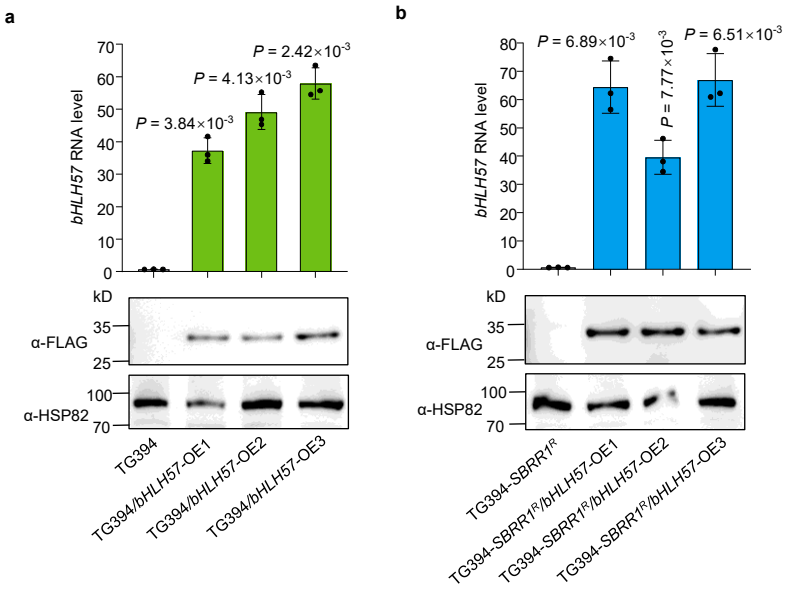

Supplementary Fig. 8. RNA and protein levels of bHLH57 in TG394/*bHLH57-OE* (a) and TG394-*SBRR1*^{R}/*bHLH57*-OE (b) transgenic lines. Upper panels represent RNA levels and lower panels are protein levels. The values represent mean ± s.d (n=3). Statistical significances were determined by a two-sided Student's *t* test. Western blots were probed with antibodies against the proteins indicated on the left sides of panels. HSP82 was used as a loading reference.

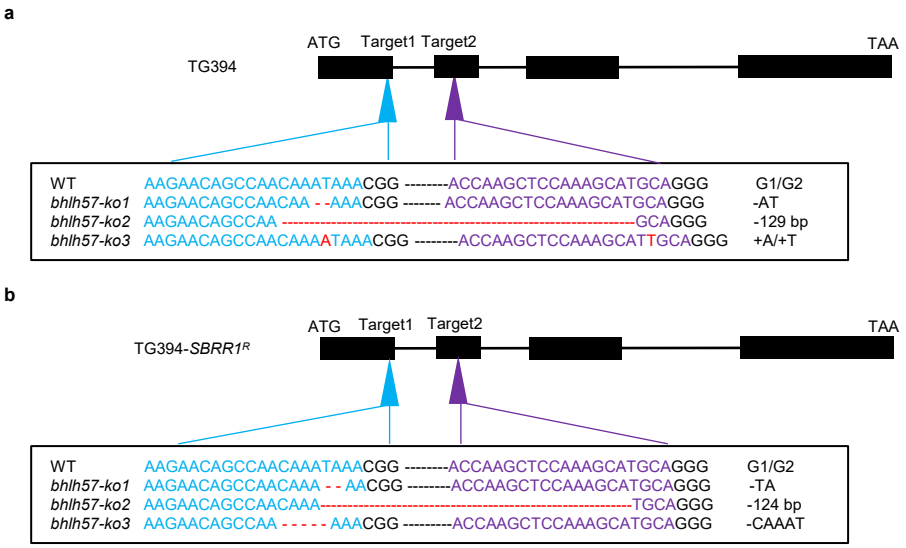

Supplementary Fig. 9. Mutation information of *bHLH57* gene in TG394/*bhlh57-ko* (a) and TG394-SBRR1^{R}/*bhlh57-ko* (b) homozygous lines. ATG represents the start codon and TAA represents the stop codon.

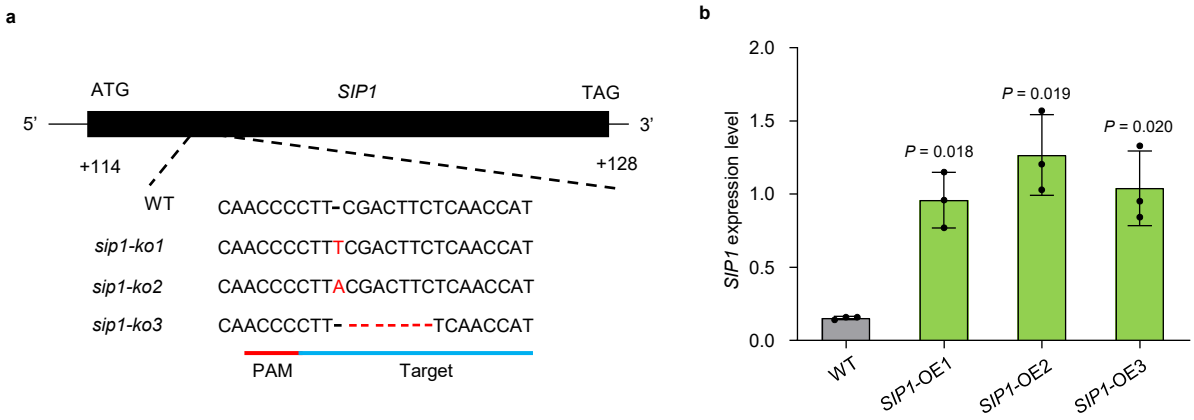

Supplementary Fig. 10. Mutation information of *SIP1* gene in homozygous knockout lines (*sip1-ko1/2/3*) (a) and expression levels of *SIP1* in WT and homozygous overexpression lines (*SIP1*-OE1/2/3) (b). The values represent mean ± s.d (n=3). Statistical significance was determined by a two-sided Student's *t* test. PAM, protospacer adjacent motif.

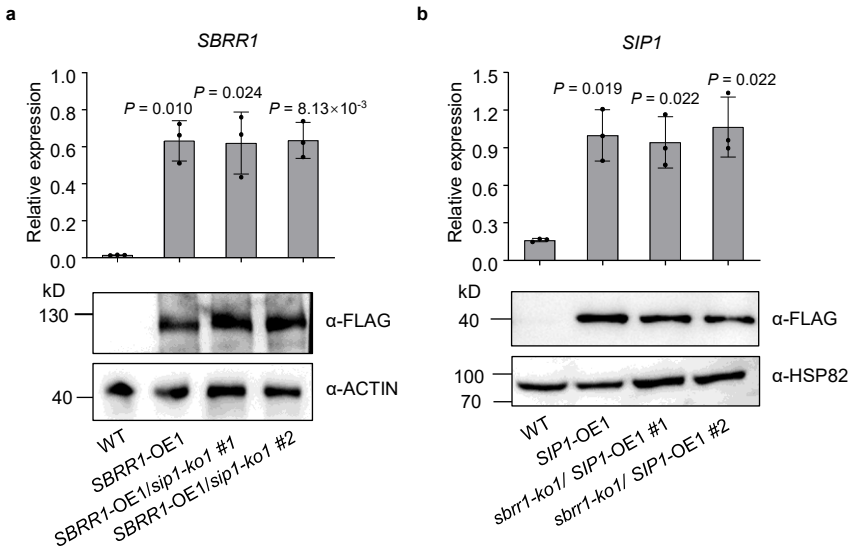

Supplementary Fig. 11. RNA and protein levels of *SBRR1* in *SBRR1*-OE1/*sip1-ko1* and *SIP1* in *sbrr1-ko1*/*SIP1*-OE1 homozygous lines. Upper panels represent RNA levels and lower panels are protein levels. The values represent mean ± s.d (n=3). Statistical significances were determined by a two-sided Student's *t* test. Western blots were probed with antibodies against the proteins indicated to the right of each panel. ACTIN was used as a loading reference.

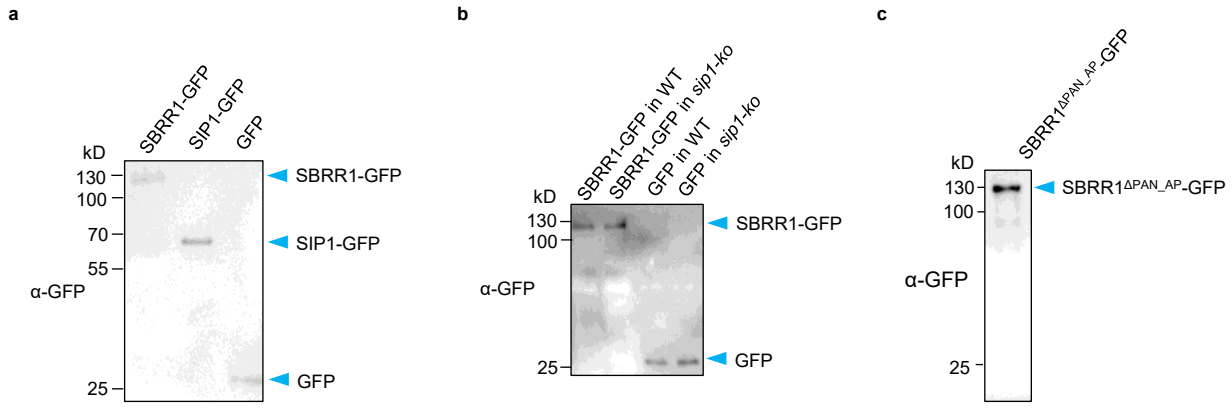

Supplementary Fig. 12. Western blot detection for the expression of full length GFP fusion proteins in rice protoplast. The proteins (labeled in the figures) used in Fig. 7a-d were probed by using a GFP antibody. Each of the GFP fusion proteins was detected essentially as a single major band representing the full-length GFP fusion protein in rice protoplasts, consistent with the predicted protein size.

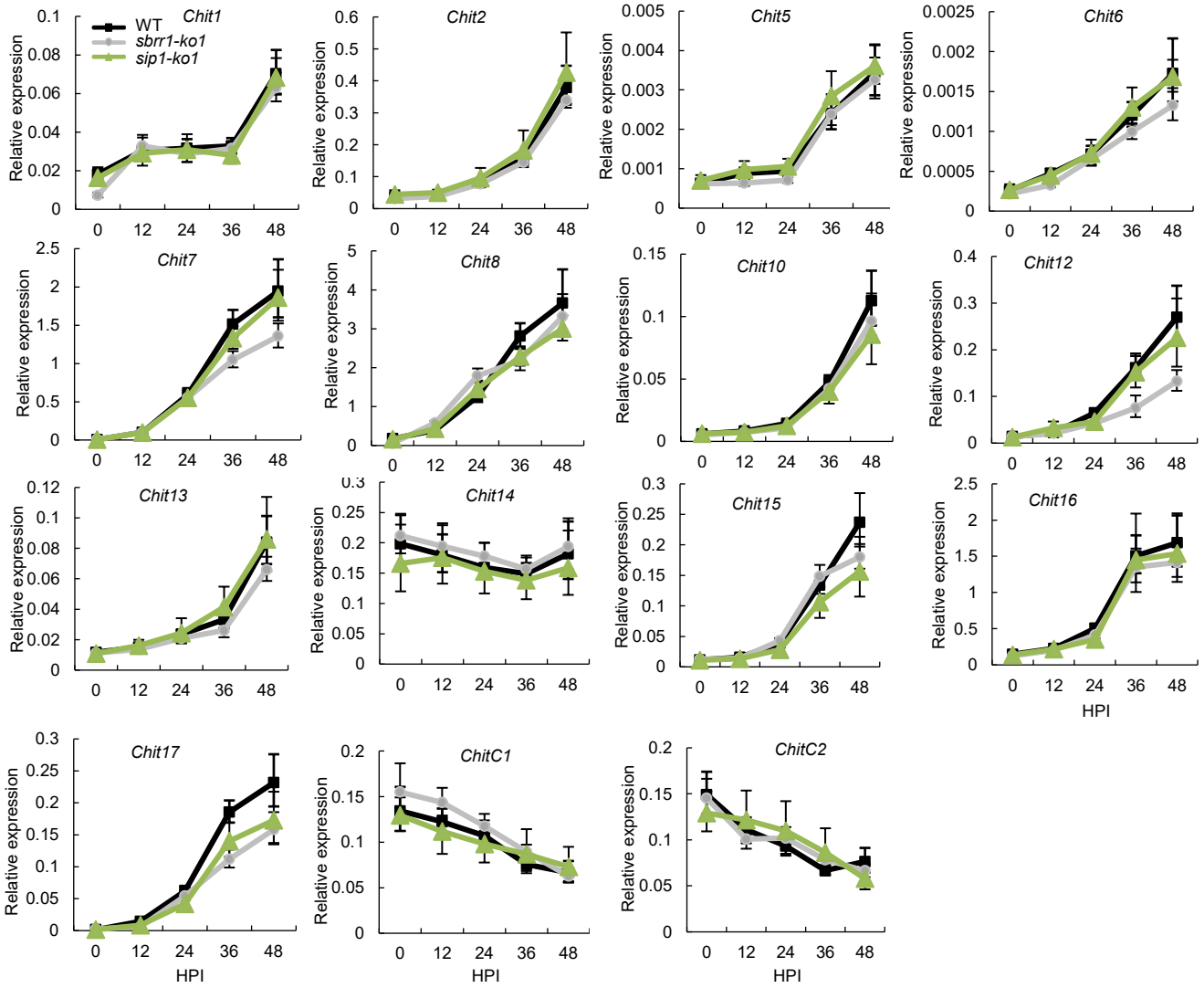

Supplementary Fig. 13. RNA expression levels of 15 other expressed chitinase genes in WT, *sbrr1-ko1* and *sip1-ko1* at different time points post *R. solani* inoculation. The values represent mean ± s.d (n=3). *Chit9* and *Chit11* are not expressed in rice leaf sheaths.

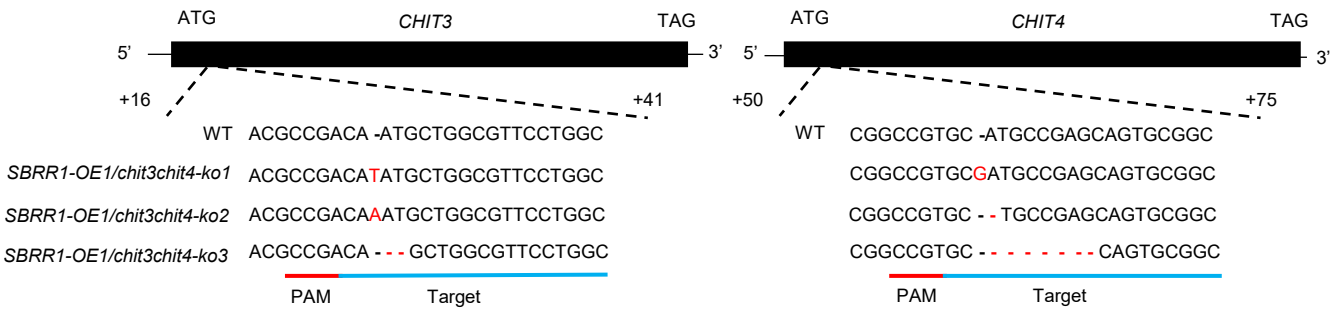

Supplementary Fig. 14. Mutation information of *Chit3* and *Chit4* genes in *chit3* and *chit4* double knockout mutants under the *SBRR1*-OE1 background.

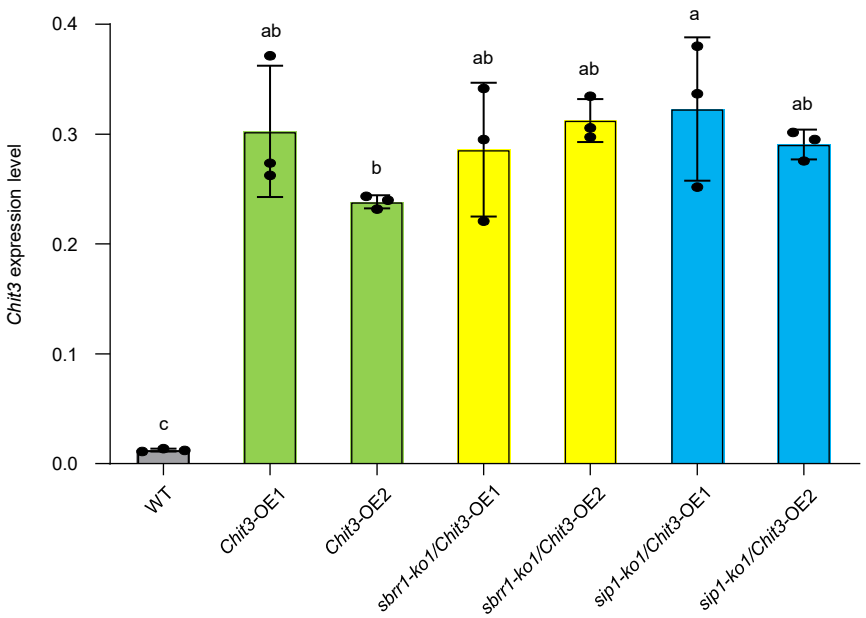

Supplementary Fig. 15. Expression levels of *Chit3* in WT, *Chit3*-OE, *sbrr1-ko1*/*Chit3*-OE and *sip1-ko1*/*Chit3*-OE homozygous lines. The values represent mean ± s.d (n=3). Different lowercase letters indicate significant differences ($P < 0.05$) based on one-way ANOVA with Duncan's multiple range tests.

Unprocessed western bolts for Supplementary Figures 2, 8, 11, 12.

Supplementary Figure 2 unprocessed western bolts

Supplementary Figure 2b

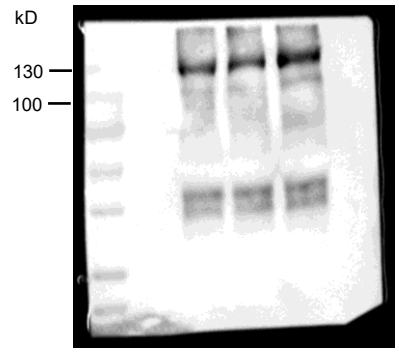

α-FLAG

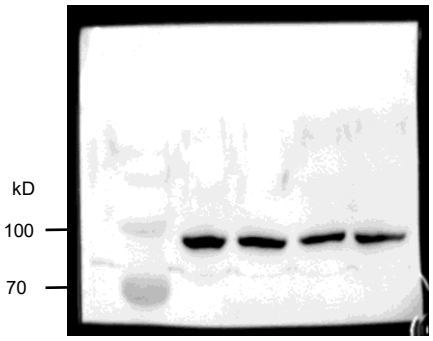

α-HSP82

Supplementary Figure 8 unprocessed western bolts

Supplementary Figure 8a

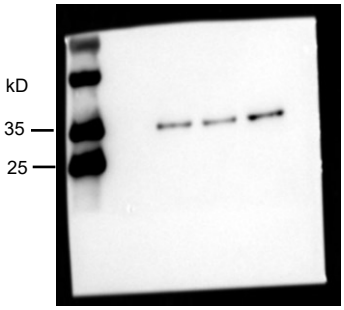

α-FLAG

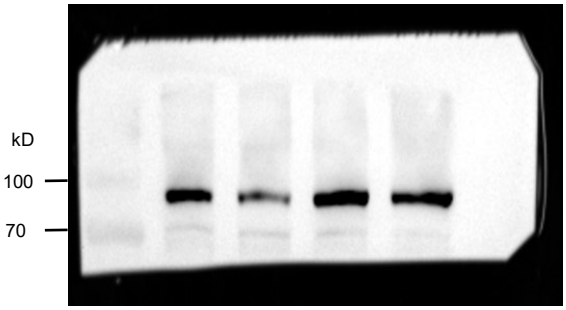

α-HSP82

Supplementary Figure 8b

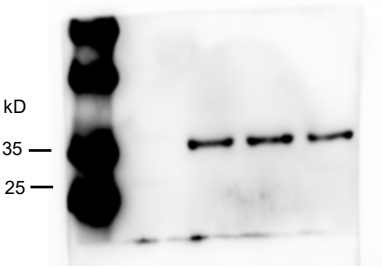

α-FLAG

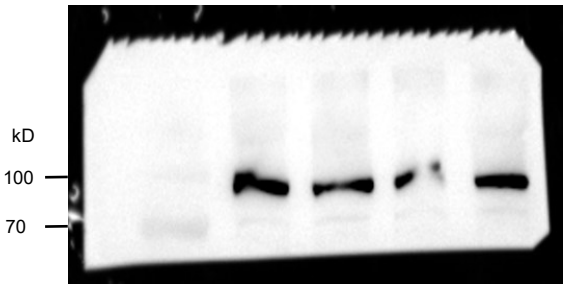

α-HSP82

Supplementary Figure 11 unprocessed western bolts

Supplementary Figure 11a

α-FLAG

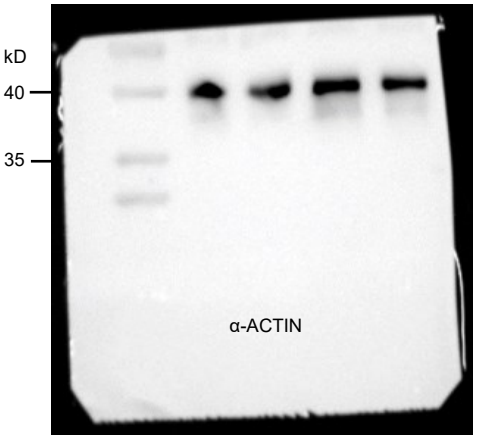

Supplementary Figure 11b

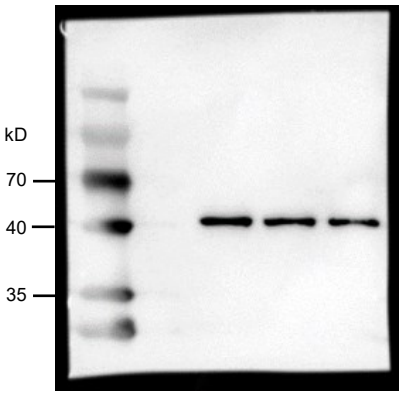

α-FLAG

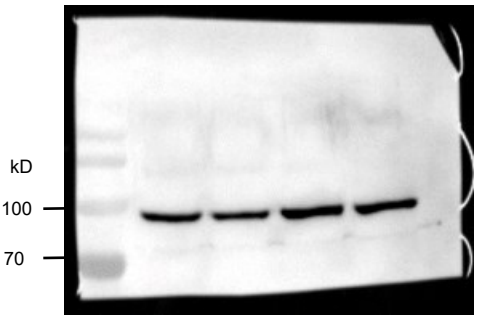

α-HSP82

Supplementary Figure 12 unprocessed western bolts

Supplementary Figure 12a

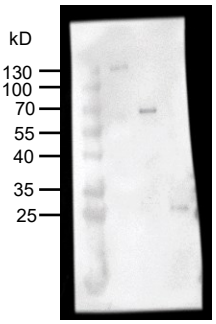

α-GFP

Supplementary Figure 12b

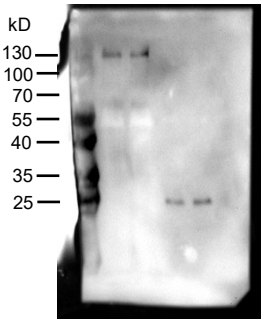

α-GFP

Supplementary Figure 12c

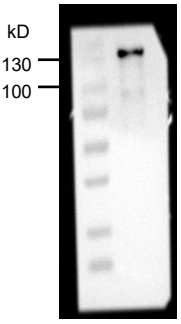

α-GFP